

Measurement of degenerate two-photon absorption spectra of a series of developed two-photon initiators using a dispersive white light continuum Z-scan

Aliasghar Ajami, Wolfgang Husinsky, Maximilian Tromayer, Peter Gruber, Robert Liska, and Aleksandr Ovsianikov

Citation: *Appl. Phys. Lett.* **111**, 071901 (2017); doi: 10.1063/1.4989917

View online: <http://dx.doi.org/10.1063/1.4989917>

View Table of Contents: <http://aip.scitation.org/toc/apl/111/7>

Published by the [American Institute of Physics](#)

Articles you may be interested in

[Broadband non-polarizing terahertz beam splitters with variable split ratio](#)

Applied Physics Letters **111**, 071101 (2017); 10.1063/1.4986538

[Magnetically-tunable cutoff in asymmetric thin metal film plasmonic waveguide](#)

Applied Physics Letters **111**, 071102 (2017); 10.1063/1.4991756

[Observation of broadband terahertz wave generation from liquid water](#)

Applied Physics Letters **111**, 071103 (2017); 10.1063/1.4990824

[Mass diffusion cloaking and focusing with metamaterials](#)

Applied Physics Letters **111**, 071903 (2017); 10.1063/1.4995600

[KF post-deposition treatment of industrial Cu\(In, Ga\)\(S, Se\)₂ thin-film surfaces: Modifying the chemical and electronic structure](#)

Applied Physics Letters **111**, 071601 (2017); 10.1063/1.4998445

[Calibration on wide-ranging aluminum doping concentrations by photoluminescence in high-quality uncompensated p-type 4H-SiC](#)

Applied Physics Letters **111**, 072101 (2017); 10.1063/1.4989648

AIP | Applied Physics
Letters

Save your money for your research.
It's now **FREE** to publish with us -
no page, color or publication charges apply.

If your article has the
potential to shape the future of
applied physics, it BELONGS in
Applied Physics Letters

Measurement of degenerate two-photon absorption spectra of a series of developed two-photon initiators using a dispersive white light continuum Z-scan

Aliasghar Ajami,^{1,2,a)} Wolfgang Husinsky,² Maximilian Tromayer,⁴ Peter Gruber,³ Robert Liska,⁴ and Aleksandr Ovsianikov³

¹Faculty of Physics, Semnan University, 35131-19111 Semnan, Iran

²Institute of Applied Physics, Vienna University of Technology, Wiedner Hauptstrasse. 8, 1040 Vienna, Austria

³Institute of Materials Science and Technology (E308), TU Wien (Technische Universität Wien), Getreidemarkt 9, 1060 Wien, Austria

⁴Institute of Applied Synthetic Chemistry, Vienna University of Technology, Getreidemarkt 9, 1060 Vienna, Austria

(Received 13 June 2017; accepted 3 August 2017; published online 15 August 2017)

To achieve efficient micro- and nanostructuring based on two-photon polymerization (2PP), the development and evaluation of specialized two-photon initiators (2PIs) are essential. Hence, a reliable method to determine the two-photon absorption (2PA) spectra of the synthesized 2PIs used for 2PP structuring is crucial. A technique by which *absolute* visible-to-near-infrared 2PA spectra of *degenerate nature* can be determined via performing a *single dispersive* white-light continuum (WLC) Z-scan has been realized. Using a dispersed white light beam containing 8 fs pulses at wavelengths ranging from 650 nm to 950 nm, the nonlinear transmittance as a function of the sample position can be measured for all spectral components by performing a *single scan* along the laser beam propagation direction. In this work, the 2PA spectrum of three different 2PIs was determined using this technique. 2PP structuring was also accomplished using the developed 2PIs at different wavelengths. Tuning the wavelength of the laser to match the peak of the 2PA spectra of the developed 2PIs resulted in lower intensity thresholds and facilitated higher structuring speeds. As an example, using M2CMK 2PI for 2PP, the scanning speed can be increased up to 5 folds when the laser wavelength is tuned to 760 nm (i.e., 2PA maximum) instead of the conventionally used 800 nm. © 2017 Author(s). All article content, except where otherwise noted, is licensed under a Creative Commons Attribution (CC BY) license (<http://creativecommons.org/licenses/by/4.0/>). [<http://dx.doi.org/10.1063/1.4989917>]

Two-photon absorption (2PA) has found many applications owing to its unique capability to induce a permanent physical/chemical change in a well-defined volume of a material, which is smaller than the focal volume given by the diffraction limit for linear absorption.¹ Consequently, it is feasible to produce 3D structures with resolution beyond the diffraction limit by means of two-photon polymerization (2PP)² or 3D grafting³ which has found applications such as in tissue engineering⁴ in the general field of biomedical engineering.⁵ In order to exploit the advantages of 2PP and advance it towards industrial applications, the throughput of the technology has to be dramatically increased. For this purpose, in addition to a higher laser pulse energy and repetition rate, specialized photoinitiators (PIs) with a higher 2PA cross section are also required. Tuning the wavelength of the laser used for structuring to match the peak of the 2PA spectra of the developed two-photon initiators (2PIs) results in greater process efficiency and consequently allows the 2PP structuring with higher throughput. Unfortunately, the linear absorption spectra do not allow us to exactly predict the 2PA behavior of PIs. One may speculate that the 2PA spectral maximum equals to twice the one-photon absorption (1PA) maximum, but there is a blue shift of the 2PA spectra relative

to the 1PA spectra since the selection rules for 2PA are different from those for 1PA.⁶ Hence, developing a reliable and fast method to determine the 2PA spectra of the synthesized 2PIs used for 2PP structuring is crucial.

For determining the 2PA spectra, a light source capable of emitting different wavelengths with sufficient intensity to induce optical nonlinearity is required. An adequate option would be a tunable laser producing ultra-short pulses [e.g., an optical parametric amplifier (OPA) or optical parametric oscillator (OPO)]. An alternative choice could be a white light continuum (WLC) source with an ultra-broadband spectrum corresponding to sub-10 fs pulses. Using such a light source in the conventional Z-scan,⁷ the 2PA cross section can be determined step by step at each wavelength. In summary, the following methods have been proposed and implemented for determining 2PA spectra:

- Using a tunable laser such as OPA or OPO: By tuning the central wavelength of the laser output, the conventional Z-scan can be repeated at different wavelengths, and thus, 2PA spectra can be obtained. This is, of course, cumbersome and time-consuming.^{8–12}
- Using a WLC¹³ source with a series of narrow band filters: In this method, a narrow range of the WLC spectrum is selected by a narrow band filter and the conventional Z-scan is performed. By changing the filter

^{a)}Author to whom correspondence should be addressed: ajami@semnan.ac.ir

and repeating the Z-scan at different wavelengths, the 2PA spectra can be obtained in a point-by-point fashion, which is again cumbersome and time-consuming.^{14–18}

- (c) Using a nondispersive WLC Z-scan: In this method, the WLC beam is focused entirely in a single spot using a spherical lens within the sample which is scanned along the laser beam direction. Therefore, both degenerate and nondegenerate 2PA (absorption of two photons at the same and different wavelengths, respectively) occur in the medium, and thus, it is impossible to determine the pure degenerate 2PA spectra using this method.^{19–21}
- (d) Using dispersive WLC without scanning: In this method, the WLC beam is spatially dispersed and then focused by a spherical lens into the sample which is mounted on the focal position. By comparing the transmission of the sample at the focus to that of the pure solvent, the relative (not the absolute) 2PA can be determined.^{22–24}

In this paper, an advanced method by which the *absolute* visible-to-near-infrared 2PA spectra of *degenerate* nature can be determined via performing a *single dispersive WLC Z-scan* is described in detail. The specific features and how to overcome the drawbacks of the aforementioned methods are presented in the following. In the setup used for this work (Fig. 1), the output pulses of a femtosecond laser amplifier at a central wavelength of 800 nm are focused at the entrance of a hollow fiber placed inside a chamber filled with argon gas (KALEIDOSCOPE™ hollow fiber compressor, Femto Lasers, Austria). The output WLC beam, which is spectrally broadened in the range of 550–1000 nm, passes through a compressor consisting of 8 chirped mirrors. The compressor provides Fourier-transform-limited pulses with a pulse duration of about 8 fs. The WLC is then spatially dispersed and collimated using a F2-glass prism-pair. The collimated spatially dispersed beam (30 mm wide and 10 mm tall) is focused by a cylindrical lens into a 50 μm tall line within the sample. In this way, the width of the beam remains unaffected, and thus, the spectral resolution does not vary when the sample is moved along the laser beam propagation direction. Since in this method different spectral components of the WLC beam are spatially separated along a narrow line inside the sample, each infinitesimal volume within the illuminated region of the sample is irradiated with a narrowband (e.g., 10 nm) radiation, leading only to degenerate 2PA originating from the same spectral components.

The transmitted intensity distribution is then imaged into a charge-coupled device (CCD) line camera [CCD-S3600-D from ALPHALAS (3648 pixels with pixel-width of

8 μm)] using a cylindrical lens. In order to prevent the saturation of the output signal of the CCD line camera, appropriate neutral density (ND) filters were used. The wavelength calibration of the CCD camera was accomplished based on the calculation results and utilizing the main amplifier beam as a reference spectrum. The data measured by each camera pixel yield the Z-scan signal for the specific spectral component. In this way, it is in principle feasible to detect 3648 Z-scan transmittance signals by performing only a single scan.

The spectrum of the transmitted spatially dispersed WLC is measured at each z-position as the sample is scanned along the beam direction. Therefore, the final measured data represent a matrix of the NM dimension. In this notation, N denotes the total number of pixels of the CCD line camera ($N = 3648$) and M denotes the number of z-positions (steps) during the entire scanning length. In the real experiment, the resolution was reduced from 0.08 nm to 5 nm by adding the signals from 60 pixels. This results in a sufficiently high signal-to-noise ratio.

By rearranging the acquired compact matrix of data, the equivalent of 60 Z-scans at different wavelengths were obtained by performing only a single scan. Figure 2(a) shows a few Z-scans at some selected wavelengths for Rhodamine B used as a standard dye to test the reliability of the method and its implementation.

The 2PA coefficient at each wavelength can be extracted by fitting Eq. (1) (Ref. 7) to the measured Z-scan for the respective wavelength.

$$T(z) = \sum_{n=0}^{\infty} \frac{(-\alpha_2 L I_0)^n}{(n+1)^{\frac{3}{2}} \left(1 + \frac{z^2}{z_R^2}\right)^n}, \quad (1)$$

where T is the normalized transmittance, L is the sample thickness, z_R is the Rayleigh range, z is the sample position measured with respect to the focal plane, I_0 is the peak on-axis intensity at the focal plane, and α_2 is the 2PA coefficient.

Then, the 2PA cross section can be calculated using the following equation:²⁵

$$\sigma_2 = \frac{hc \alpha_2}{\lambda N_A \rho \times 10^{-3}}, \quad (2)$$

where h is the Planck constant, c is the light speed in free space, N_A is the Avogadro constant, ρ is the concentration of the examined solution in mol/lit, and λ is the wavelength.

The CCD output signal was then calibrated with respect to the sensitivity curve of the CCD and the transmission

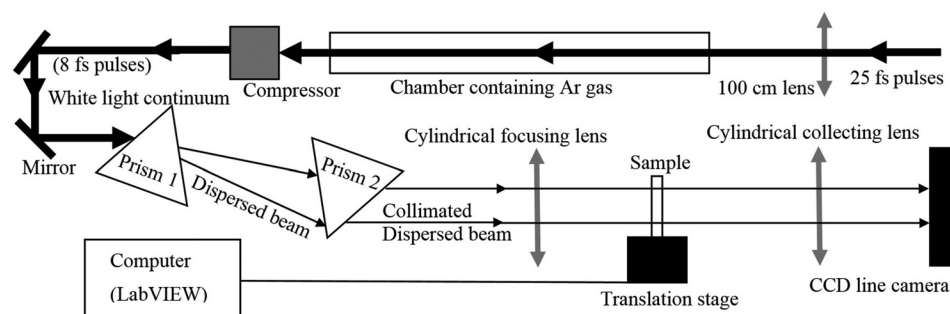


FIG. 1. Setup of the dispersed white light Z-scan.

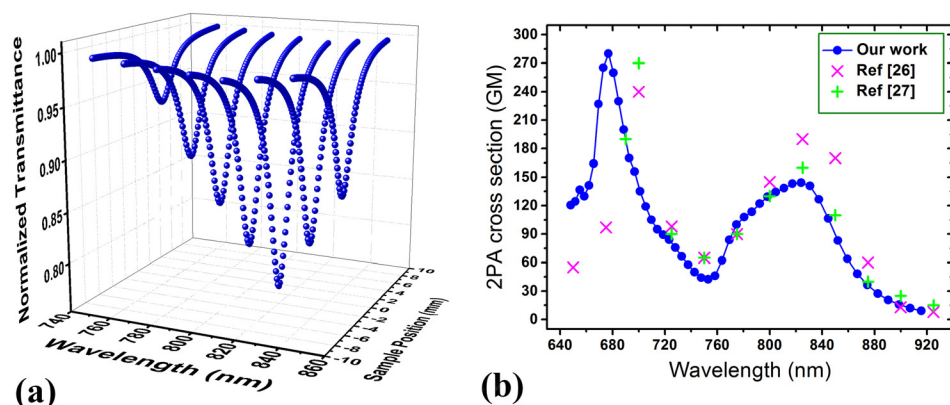


FIG. 2. (a) Selected Z-scan curves of Rhodamine B measured at different wavelengths (data fit). (b) 2PA spectra of Rhodamine B; the solid circles indicate the data measured in our work, while the crosses indicate the values taken from the literature.

curve of the ND filters. Then, the spectral energy can be determined using $(dI/\Delta I)E$, where dI is the summation of intensity detected by each of the adjacent 60 pixels, ΔI is the summation of intensity detected by all 3600 pixels when the sample is far away from the focal plane, and E is the entire pulse energy that was measured prior to the prism pair. By determining the energy for each spectral region, the magnitude of I_0 required for fitting Eq. (1) to the Z-scan is obtained.

In order to test and verify this method, Rhodamine B was measured since it is one of the few materials for which the 2PA spectra can be found in the literature. Figure 2(b) illustrates the 2PA spectra of Rhodamine B, indicating a peak 2PA around 820 nm, which is in a reasonable agreement with the data found in the literature.^{26,27}

A few recently developed 2PIs have been examined using the proposed technique. The organosoluble 2PI M2CMK²⁸ is typically used for submicrometre stereolithography and rapid prototyping using acrylate resins, whereas P2CK and E2CK²⁹ are water-soluble and were developed to facilitate the printing of hydrogel scaffolds for tissue engineering.

Figure 3 shows the 2PA spectra of the selected 2PIs obtained by our method.

The water-soluble initiator P2CK shows the largest 2PA cross section as compared to other initiators with the main peak around 810 nm. The second water soluble initiator E2CK has its main absorption peak at 830 nm. M2CMK possess a broad absorption band ranging from 700 nm to 850 nm with the main peak around 760 nm.

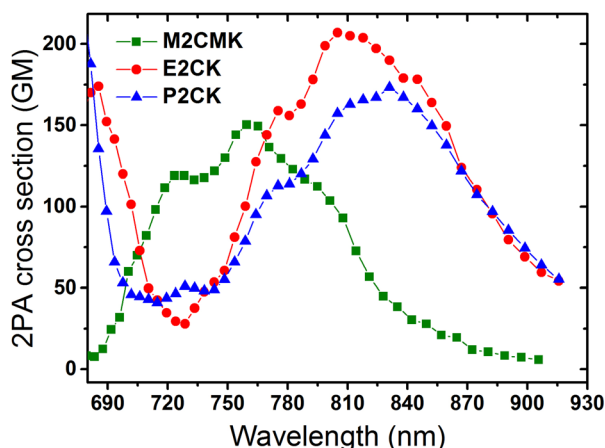


FIG. 3. 2PA spectra of three different 2PIs (M2CMK, P2CK, and E2CK) measured using the developed method.

3D polymeric structures were produced in a solution of the 2PI dissolved in a 1:1 equimolar mixture of trimethylolpropane triacrylate (TTA, Genomer 1330) and ethoxylated-(20/3)-trimethylolpropane triacrylate (ETA, Sartomer 415). The sample is mounted on an assembly of three linear translation stages for complete 3D movement. A tunable femtosecond laser oscillator (MaiTai DeepSee by Spectra Physics) was used for 2PP structuring. An acousto-optical modulator was employed for fast switching of the laser beam and for adjusting its intensity. The beam was focused into the sample with a water-immersion microscopy objective (32x/NA = 0.85). The woodpile structures were created by scanning the beam within the sample by using a galvo scanner (HurryScan, ScanLab).

Figures 4(a) and 4(b) show the laser scanning microscopy (LSM) images of the 3D polymeric structures created based on 2PP using M2CMK applying two different wavelengths of 760 nm and 800 nm, respectively. In both tests, the laser power varied in the range of 4–22 mW and the writing speed varied in the range of 20–200 mm/s. At the lowest scanning speed of 20 mm/s, a laser power of 6 mW is sufficient to produce defect-free structures using 760 nm, whereas 8 mW is still not sufficient to create the same structure using 800 nm. It can be asserted that the power threshold is reduced by more than 20% using 760 nm instead of 800 nm. This observation is in good agreement with the 2PA spectra shown in Fig. 3, explained by the fact that the energy absorbed in the 2PA process is proportional to the product of the 2PA cross section and the square of the laser intensity. Tuning the laser wavelength to match the 2PA peak of M2CMK resulted in a possible increase in the writing speed. By comparing Figs. 4(a) and 4(b), one can recognize that in the power range of 8–10 mW, the writing speed can be increased by a factor of at least 5 using 760 nm instead of 800 nm. For instance, at a laser power of 10 mW, the scanning speed should be less than 40 mm/s to produce a defect-free structure using 800 nm, whereas the scanning speed can be increased up to 200 mm/s using 760 nm wavelengths. This can be understood because 10 mW is just above the threshold using 800 nm, while for 760 nm, 10 mW is substantially above the threshold and consequently leads to producing much more polymer, thus allowing a substantial increase in the scanning speed. The developed method provides means to screen spectral 2PA characteristics of different compounds in a quick and reliable manner. The obtained data can serve as a guideline for the design of specialized 2PIs. It has to be noted that, while the change in the 2PP threshold values was

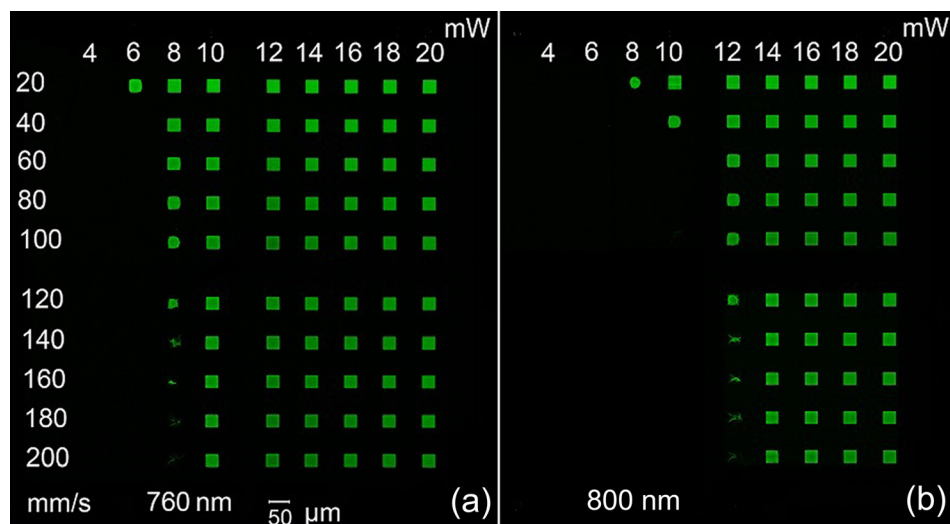


FIG. 4. LSM images of 3D polymeric structures created based on 2PP using M2CMK applying two different wavelengths of 760 nm (a) and 800 nm (b). The values along the horizontal axis indicate the laser power in mW, and the column on the left indicates the structuring speed in mm/s.

observed, additional methods have to be used in order to verify the resulting double-bond conversion within the 2PP produced structures.³⁰

In conclusion, we have shown that the *absolute* visible-to-near-infrared 2PA spectra of *degenerate* nature of nonlinear materials can be determined in a quick and reliable manner by a single scan. A WLC produced by a hollow fiber was used to measure the 2PA spectrum of a few selected 2PIs in the range of 650–950 nm from which the peak 2PA for each 2PI was determined. In order to verify the result of the 2PA spectral measurement, 3D structuring based on 2PP was also realized using the examined 2PIs at different wavelengths delivered by a tunable laser. The 2PP results using the examined 2PIs were consistent with the 2PA spectrum: (1) the power threshold to induce 2PP decreases with the increasing 2PA cross section of the 2PI and (2) tuning the wavelength of the laser to match the peak of the 2PA spectra allows producing 2PP structures at significantly higher scanning speed (e.g., more than 5 times higher in our work).

This work was supported by Austrian Science Fund (FWF) with Project No. 27555-N28.

¹R. Liska, J. Stampfl, and A. Ovsianikov, *Multiphoton Lithography: Techniques, Materials, and Applications* (Wiley, 2016).

²M. Emons, K. Obata, T. Binhammer, A. Ovsianikov, B. N. Chichkov, and U. Morgner, *Opt. Mater. Express* **2**, 942 (2012).

³A. Ovsianikov, Z. Li, A. Ajami, J. Torgersen, W. Husinsky, J. Stampfl, and R. Liska, *Appl. Phys. A: Mater. Sci. Process.* **108**, 29 (2012).

⁴M. S. Hahn, J. S. Miller, and J. L. West, *Adv. Mater.* **17**, 2939 (2005).

⁵A. Ovsianikov, V. Mironov, J. Stampf, and R. Liska, *Expert Rev. Med. Devices* **9**, 613 (2012).

⁶M. Drobizhev, N. S. Makarov, S. E. Tillo, T. E. Hughes, and A. Rebane, *Nat. Methods* **8**, 393 (2011).

⁷M. Sheik-Bahae, A. A. Said, T.-H. Wei, D. J. Hagan, and E. W. Van Stryland, *IEEE J. Quantum Electron.* **26**, 760 (1990).

⁸M. G. Vivase, D. L. Silva, L. Misoguti, R. Zalesny, W. Bartkowiak, and C. R. Mendonca, *J. Phys. Chem. A.* **114**, 3466 (2010).

⁹D. S. Corrêa, S. L. Oliveira, L. Misoguti, S. C. Zilio, R. F. Aroca, C. J. L. Constantino, and C. R. Mendonça, *J. Phys. Chem. A.* **110**, 6433 (2006).

¹⁰U. M. Neves, L. De Boni, Z. Ye, X. R. Bu, and C. R. Mendonça, *Chem. Phys. Lett.* **441**, 221 (2007).

¹¹C. R. Mendonca, D. S. Correa, T. Baldacchini, P. Tayalia, and E. Mazur, *Appl. Phys. A: Mater. Sci. Process.* **90**, 633 (2008).

¹²L. De Boni, A. A. Andrade, L. Misoguti, S. C. Zilio, and C. R. Mendonça, *Opt. Mater.* **32**, 526 (2010).

¹³R. R. Alfano and S. L. Shapiro, *Phys. Rev. Lett.* **24**, 592 (1970).

¹⁴M. Balu, L. A. Padilha, D. J. Hagan, E. W. Van Stryland, S. Yao, K. Belfield, S. Zheng, S. Barlow, and S. Marder, *J. Opt. Soc. Am. B: Opt. Phys.* **25**, 159 (2008).

¹⁵M. Balu, J. Hales, D. Hagan, and E. Van Stryland, *Opt. Express* **13**, 3594 (2005).

¹⁶M. Balu, J. Hales, D. Hagan, and E. Van Stryland, *Opt. Express* **12**, 3820 (2004).

¹⁷S. L. Oliveira, D. S. Corrêa, L. De Boni, L. Misoguti, S. C. Zilio, and C. R. Mendonça, *Appl. Phys. Lett.* **88**, 021911 (2006).

¹⁸M. Balu, J. Hales, D. J. Hagan, and E. W. Van Stryland, paper presented at the Optics InfoBase Conference Papers, 2006.

¹⁹B. Anand, N. Roy, S. Siva Sankara Sai, and R. Philip, *Appl. Phys. Lett.* **102**, 203302 (2013).

²⁰S. Perumbilavil, P. Sankar, T. Priya Rose, and R. Philip, *Appl. Phys. Lett.* **107**, 051104 (2015).

²¹L. De Boni, A. Andrade, L. Misoguti, C. Mendonça, and S. Zilio, *Opt. Express* **12**, 3921 (2004).

²²G. S. He, T.-C. Lin, P. N. Prasad, R. Kannan, R. A. Vaia, and L.-S. Tan, *J. Phys. Chem. B* **106**, 11081 (2002).

²³G. S. He, T. C. Lin, J. Dai, P. N. Prasad, R. Kannan, A. G. Dombroskie, R. A. Vaia, and L. S. Tan, *J. Chem. Phys.* **120**, 5275 (2004).

²⁴G. He, T.-C. Lin, P. Prasad, R. Kannan, R. Vaia, and L.-S. Tan, *Opt. Express* **10**, 566 (2002).

²⁵B. A. Reinhardt, L. L. Brott, S. J. Clarson, A. G. Dillard, J. C. Bhatt, R. Kannan, L. Yuan, G. S. He, and P. N. Prasad, *Chem. Mater.* **10**, 1863 (1998).

²⁶N. S. Makarov, M. Drobizhev, and A. Rebane, *Opt. Express* **16**, 4029 (2008).

²⁷C. Xu and W. W. Webb, *J. Opt. Soc. Am. B: Opt. Phys.* **13**, 481 (1996).

²⁸Z. Li, N. Pucher, K. Cicha, J. Torgersen, S. C. Ligon, A. Ajami, W. Husinsky, A. Rosspeintner, E. Vauthey, S. Naumov, T. Scherzer, J. Stampfl, and R. Liska, *Macromolecules* **46**, 352 (2013).

²⁹Z. Li, J. Torgersen, A. Ajami, S. Muhleder, X. Qin, W. Husinsky, W. Holthöner, A. Ovsianikov, J. Stampfl, and R. Liska, *RSC Adv.* **3**, 15939 (2013).

³⁰K. Cicha, Z. Li, K. Stadlmann, A. Ovsianikov, R. Markut-Kohl, R. Liska, and J. Stampfl, *J. Appl. Phys.* **110**, 064911 (2011).